

Light propagation in the micro-size capillary injected by high temperature liquid*

LI Yan-jun (李艳军)^{1,2}, Edward LI (李士阳)^{1,3}, and XIAO Hai (肖海)^{1**}

1. The Holcombe Department of Electrical and Computer Engineering, Clemson University, Clemson 29634, USA

2. College of Electrical Engineering, Henan University of Technology, Zhengzhou 450001, China

3. Sciences and Mathematics, Furman University, Greenville 29613, USA

(Received 22 June 2016; Revised 26 September 2016)

©Tianjin University of Technology and Springer-Verlag Berlin Heidelberg 2016

The high temperature liquid is injected into the micro-size capillary and its light propagation behavior is investigated. We focus on two different liquid pumping methods. The first method can pump the high temperature liquid tin into the micro-size capillary by using a high pressure difference system. After pumping, a single mode fiber (SMF) connected with the optical carrier based microwave interferometry (OCMI) system is used to measure different liquid tin levels in the micro-size capillary. The second method can pump the room temperature engine oil into the capillary by using a syringe pump. This method can avoid the air bubbles when the liquids are pumped into the capillary.

Document code: A **Article ID:** 1673-1905(2016)06-0405-4

DOI 10.1007/s11801-016-6144-9

Optical fiber-based devices^[1-5] are widely used in optical communications and sensing applications. The diameters of some optical capillary tubes are close to those of optical fibers, so it is easy to fuse an optical capillary tube with the optical fiber together, to form an optical fiber & capillary-based sensor by using a fusion splicer^[6,7]. This kind of sensor can pump liquids into it, which has a great potential in embedded sensor and optical coherence tomography applications^[8,9]. However, the inner diameter (ID) of the capillary tube is around micrometers, and the capillary force and the wettability will prevent the liquids^[10], especially for the high temperature metal liquids pumped into the hollow core of the capillary tube. Myung Sup Yoon et al^[11] installed an asymmetric electrode array on the top and bottom walls of the micro-channel, and the electro-osmotic micro-channel flow driven by arrays of alternating current (AC) asymmetric electrodes was carried out to generate the pumping mode of the liquid flow. This method could pump the liquids into the micro-channel and control the liquid flow. However it's hard to pump the high temperature liquids into the capillary, which may destroy the electrodes. Junya Ogawa et al^[12] proposed a new mechanical micro-pumping device for microfluidic system, which used a vibration channel wall. However, if the capillary tube is too long, there may be air bubbles in the micro-channel. In this paper, we focus on two different methods to pump high temperature metal liquids and avoid air bubbles in the optical fiber and capillary-based sensor, respectively. Furthermore, an optical carrier based microwave inter-

ferometry (OCMI) system is used to measure the optical signals in this sensor.

In this method, the optical fiber & capillary-based sensor consists of three parts: the reservoir, capillary tube, and a single mode fiber (SMF). The reservoir was fused together with the tube through a fusion splicer. The other end of the tube was fused with the SMF. A 70- μm ID empty core is used as the tube where the liquid tin level could be measured, and a 150- μm outer diameter (OD) cladding capillary is used as the reservoir for holding the liquid tin.

In order to pump the high temperature liquid tin into the optical fiber and capillary-based sensor, a pressure difference pump mechanism is utilized. The pump mechanism utilizes a stainless steel gas chamber that was assembled in the lab as shown in Fig.1. A 1" steel cap was screwed onto a 1" steel tube with about 10 cm in length. A reducer was then attached to the 1" tube to connect with a 3/8" steel tube, which in turn was connected to a 1/4" steel tube for about 22 cm. At the top of the 1/4" steel tube, two 3-way air way connectors were attached: One was attached directly to the 1/4" steel tube where a rubber stopper was placed and plugged with a small cap, while the other was connected to the first 3-way connector on the side. The second 3-way connector was attached to two valves: One was connected to an Ar gas tank with a pressure meter, while the other acted as a pressure release. The steel chamber was put inside an oven. At the bottom of the chamber, a small crucible was placed to hold a tin block. A hole was drilled at the cen-

* This work has been supported by the U.S. Department of Energy, National Energy Technology Laboratory, Morgantown, WV, USA (No. DE-FE0012272), and the Joint Funds (NSFC-Henan) of the National Natural Science Foundation of China (No.U1204615).

** E-mail:haix@clemson.edu

ter of the tin block to let the sensor pass through.

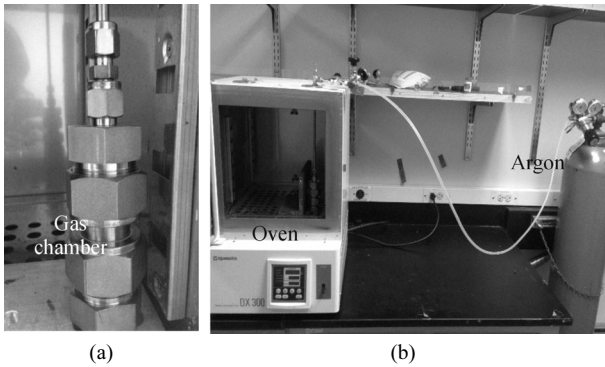


Fig.1 (a) Stainless steel gas chamber; (b) The entire setup

The 20- μm ID capillary tube was fused with the 75- μm ID reservoir both ends of which are left open-ended. Using a needle, the structure was gently inserted through the rubber stopper and into the steel chamber until it went through the hole in the tin block and barely touched the bottom of the crucible. The needle was pulled out of the rubber stopper and stringed off the sensor. The system was then tightly shut and the oven was closed. The oven was turned on up to 310 $^{\circ}\text{C}$ for 5 min for the tin melting. After the tin melted, the argon was gradually pumped into the chamber up to 1.034×10^6 Pa for 40 min to 60 min. The oven was turned off and the capillary was pulled out and sealed at the reservoir end. The structure was taken to the microscope for analysis.

This system used the argon gas to prevent the unwanted oxidation the tin might undergo. If tin is converted to tin oxide or tin dioxide, the melting temperature would exceed that of silica, thus it would be unusable as a sensing material. On one end, argon gas was pumped from a tank through a series of plastic tubes which were connected to a flow meter and a drierite. The gas then flowed into a syringe and needle that directly fed into the capillary tube. On the other end, another series of plastic tubes were connected to the in-house vacuum system and a flow meter, which in turn fed into the capillary tube. Both needles and the sensor itself were locked in place with a rubber stopper which was used to close the entire system. The system was first vacuumed in order to create negative pressure inside the sensor and the chamber was heated by the oven. After the tin block has melted and the sensor end has been submerged inside the liquid tin, argon was slowly added into the system to pump the liquid tin into the reservoir.

The reservoir was connected to a 20- μm ID empty core and 150- μm OD cladding silica tube, where the liquid tin levels reading took place. Because tin has a stronger cohesive force than adhesive force against glass^[13,14], the meniscus has a convex shape due to the cohesive forces drawing the liquid tin into a drop. In this way, the liquid tin will not bind to the wall of the capillary and can freely move according to the temperature it

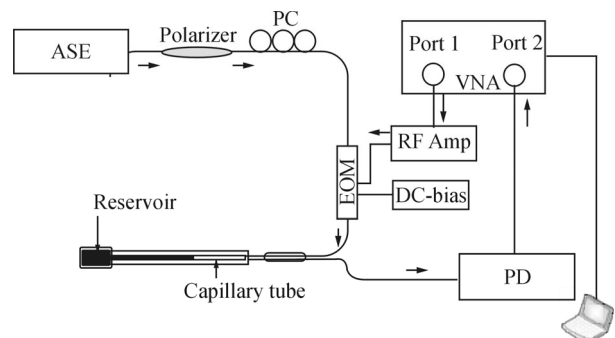
experiences. The average expansion coefficient^[15] was proved to be $\gamma = 113 \times 10^{-6}/^{\circ}\text{C}$ between 300 $^{\circ}\text{C}$ and 1 600 $^{\circ}\text{C}$. In 1966, Doge^[16] measured the actual volumetric expansion coefficients at 240 $^{\circ}\text{C}$ and 1 200 $^{\circ}\text{C}$ are $\gamma = 105 \times 10^{-6}/^{\circ}\text{C}$ and $\gamma = 96 \times 10^{-6}/^{\circ}\text{C}$, respectively. Due to this large difference in volumetric expansion coefficients, the temperature range for the sensor is between 500 $^{\circ}\text{C}$ and 1 000 $^{\circ}\text{C}$ for accurate measurement of temperature. The ratio between the lengths of the reservoir and the tube is expressed as

$$\frac{L_{\text{reservoir}}}{L_{\text{tube}}} = \frac{\pi \cdot ID_{\text{tube}}^2}{\Delta T \cdot \gamma \cdot \pi \cdot ID_{\text{reservoir}}^2} = \frac{1}{1.1}, \quad (1)$$

where ID_{tube} and $ID_{\text{reservoir}}$ are the inner diameters of the tube and the reservoir, respectively, ΔT is the temperature range and γ is the average of the volumetric expansion coefficients at 240 $^{\circ}\text{C}$ and 1 200 $^{\circ}\text{C}$.

A 20-cm-long 20- μm ID capillary and 15.3-cm-long 70- μm ID capillary were used for the tube and the reservoir, respectively. This ratio of the reservoir length to tube length is 1/1.3. The experimental length ratio is different from that in Eq.(1), because the temperature range used is between 300 $^{\circ}\text{C}$ and 500 $^{\circ}\text{C}$.

After the sensor was filled with liquid tin and sealed, the open end of the SMF was connected to the OCMI system shown in Fig.2. The light passed through the SMF into the tube where the light will reflect off the liquid tin level. The reflected light will be sent back to the OCMI where the reflected wavelength of the light will be compared with the base wavelength of 1 550 nm. Then, we can obtain the time delay between the reflected and base wavelengths. Since the liquid tin level in the tube changes with temperature due to the thermal expansion coefficient of liquid tin, there will be a unique time delay associated with each temperature reading. In this way, we can accurately calibrate the time delay of OCMI and the sensor to the standard temperature reading.



ASE: amplified spontaneous emissions or light source; PC: polarization controller; EOM: electro-optical modulator; PD: photodetector; VNA: vector network analyzer; RF Amp: radio frequency amplifier

Fig.2 The OCMI system

The second sensor used the 75- μm ID empty core and 150- μm OD cladding capillary as a reservoir connected to a 10- μm ID hollow core and 150- μm OD cladding silica tube. The majority of the sensor was filled with

engine oil, only leaving an air bubble length around 300 μm , one end of which would always be the fusion point between the tube and the SMF. This seems to be less effective than the first model, because the internal pressure will cause a nonlinear relationship between the changes in temperature and bubble length. However, this method we propose can ensure that the areas filled with either air or engine oil have a uniform distribution of the solution. Furthermore, if a solid or a viscous liquid is used as the sensing material in the first method, the possibility of uneven or nonlinear expansion due to impurities will be introduced during pumping.

During fabrication, a 10-mm-long 75- μm ID reservoir was fused with a 30-mm-long 10- μm ID tube. A syringe pump was epoxied to the reservoir end and pumped engine oil in the sensor at a rate of 5 $\mu\text{L}/\text{min}$. The engine oil was pumped until it was close to 300 μm , then the 10- μm ID tube was fused with an SMF. More oil was pumped to make the air bubble be 300 μm in length. The SMF was connected to the OCMI in order to detect reflection at both ends of the bubble.

In order to amplify the reflected signal, two different types of fusion modes were performed at the fusion point between the 10- μm ID tube and the SMF. They are flat and cone shape fusion modes respectively as shown in Fig.3. For the flat fusion, a 10- μm ID tube and an SMF were fused by a short electrical splice of about 5 s. For the cone-shape fusion, a 10- μm ID tube was embedded in an SMF and concaved towards the air bubble.

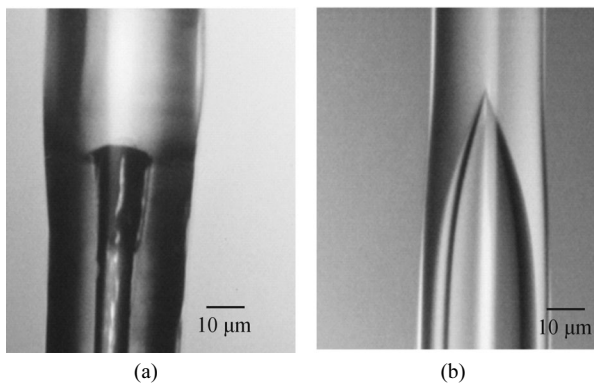


Fig.3 Two fusion types between the 10- μm ID tube and SMF:(a) Flat fusion; (b) Cone-shape fusion

After different sensors were fabricated and tested for reflected signals, a gold metallic coating was applied on the sensor. The sensor was coated with gold in order to increase the reflectivity of the propagating light and to restrict the amount of light that was escaping through the cladding. The coating covered from the end of the fusion point on the MMF to a length beyond the end of the air bubble in the tube. The sensors were tested again to compare the reflected signals between the coated sensor and the uncoated one.

When the optical fiber & capillary-based sensor was well sealed in the stainless steel chamber, the chamber

was first vacuumed to produce negative pressure inside the sensor to prevent unwanted oxidation of the tin. Then the oven was turned on up to 310 $^{\circ}\text{C}$ for 5 min for the tin melting. After that, the argon was gradually pumped into the chamber up to 1.034×10^6 Pa for 40 min to 60 min. The oven was turned off and the capillary was pulled out and sealed at the reservoir end. The stainless steel gas chamber was able to successfully pump liquid tin into the sensor. However, there are two main issues with this setup. First, we could not observe the pump action in real time, so everything has to be in place and timed correctly. The second is that isolated pockets of argon bubbles were stuck between long tin sections inside the tubes. Images of the resulting sensor are shown in Fig.4. It is clearly shown that the high temperature liquid tin was successfully pumped into the 15.3-cm-long 75- μm ID capillary, then passed the fusion point of 20- μm and 75- μm ID capillaries into the 20- μm ID capillary tube successfully more than 13 cm in length.

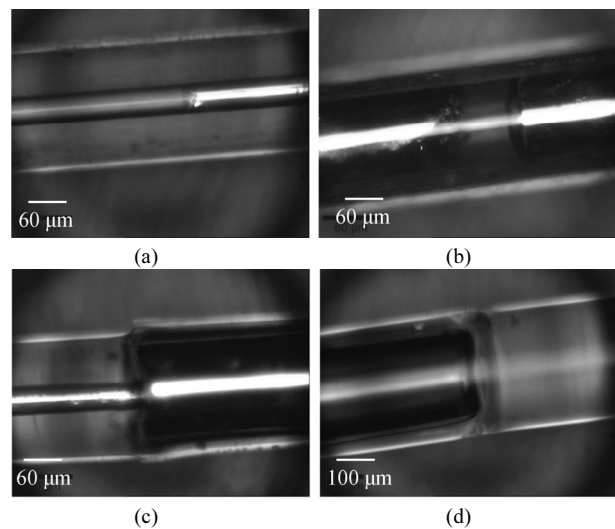


Fig.4 (a) 20- μm ID capillary filled with tin; (b) 75- μm ID capillary filled with air gap between tin segments; (c) The fusion point of 20- μm and 75- μm ID capillaries filled with tin; (d) 75- μm ID capillary fused with a single mode fiber

A 10-mm-long 75- μm ID reservoir was fused with a 30-mm-long 10- μm ID tube. A syringe pump was epoxied to the reservoir end, and the engine oil was pumped into this sensor at a rate of 5 $\mu\text{L}/\text{min}$. We are able to pump the engine oil into both ends of the sensor and pass the fusion point between the 75- μm ID reservoir and the 10- μm ID tube, which is shown in Fig.5. It is clear that we have successfully avoided the air bubble to be pumped into the 10- μm ID tube during the engine oil pumping.

After successfully pumping the engine oil into the sensor, the open end of the SMF was connected to the OCMI system to detect the reflected signal from the fusion point and the liquid level. Two different types of fusion modes (flat and cone-shape fusion modes) were

performed at the fusion point between the 10- μm ID capillary tube and the SMF, mentioned in Fig.3. The optical light reflection results are shown in Fig.6.

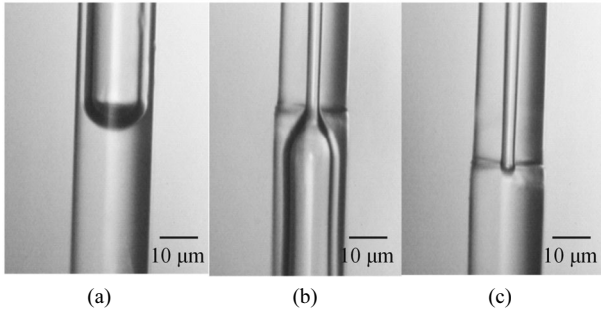


Fig.5 (a) 75- μm ID reservoir with oil; (b) Oil passing through the fusion point of 75- μm ID and 10- μm ID capillaries; (c) 10- μm ID capillary filled with engine oil

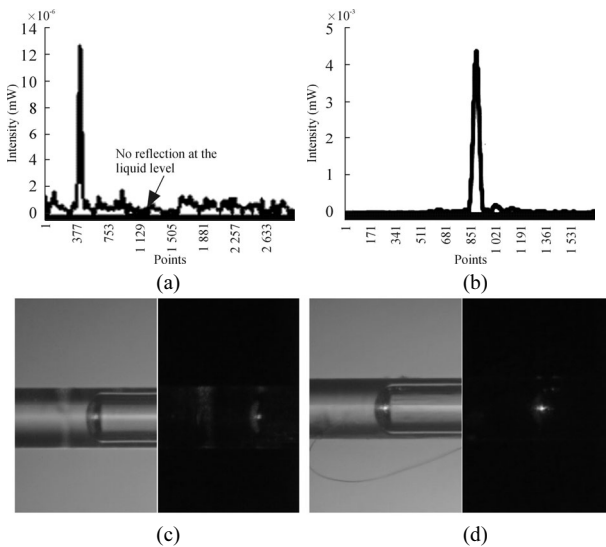


Fig.6 (a) Cone shape fusion reflection; (b) Flat fusion reflection; Reflection of the liquid level in the hollow core and scattering in the wall of the capillary tube for (c) cone fusion and (d) flat fusion

We can see from Fig.6(a) and (b) that the cone-shape fusion point has lower reflection, which means higher optical light transmission to the optical capillary tube. However, more optical light from the SMF will transmit into the wall of the capillary tube in cone-shape fusion mode than that in flat fusion mode. In this case, the optical light will greatly decrease when transmits in the hollow core of the capillary tube. Comparing Fig.6(c) and (d), we can see that the optical light transmitting in the hollow core of the capillary tube will decrease greatly for the cone-shape fusion mode than that for the flat fusion mode.

In this paper, we have successfully pumped the high temperature liquid tin and the engine oil into the optical fiber & capillary-based sensor by setting up an argon gas pressure difference system. We could pump the high temperature liquid tin into the capillary for more than 30 cm in length. The small volume structure of this sen-

sor filled with liquid tin has great potential to make a high temperature optical thermometer. This thermometer may be embedded in the high temperature object to achieve real-time monitoring. We also introduced an SMF connected with the OCMI system to measure the different liquid levels in the micro-size capillary. We successfully fused the capillary tube and the fiber with flat shape and cone shape. We find that the intensity of the optical light transmitting in the cone shape structure of the optical fiber will decrease greatly than that in the flat shape one.

References

- [1] BIAN Ji-cheng, LANG Ting-ting, YU Wen-jie and KONG Wen, Journal of Optoelectronics-Laser **26**, 2169 (2015). (in Chinese)
- [2] López-Higuera José Miguel, Rodriguez Cobo Luis, Quintela Incera Antonio and Cobo Adolfo, Journal of Lightwave Technology **29**, 587 (2011).
- [3] CAO Ye, LIU Wen, ZHAO Shun, TONG Zheng-rong and LIU Hui-ying, Journal of Optoelectronics · Laser **26**, 1233 (2015). (in Chinese)
- [4] Yanjun Li, Tao Wei, John A. Montoya, Sandeep V. Saini, Xinwei Lan, Xiling Tang, Junhang Dong and Hai Xiao, Applied Optics **47**, 5296 (2008).
- [5] Wei T., Han Y., Li Y., Tsai H. L. and Xiao H., Optics Express **16**, 5764 (2008).
- [6] Hanzheng Wang, Xinwei Lan, Jie Huang, Lei Yuan, Cheolwoon Kim and Hai Xiao, Optics Express **21**, 15834 (2013).
- [7] X. Fan and I. M. White, Nat. Photonics **5**, 591 (2011).
- [8] Nemiroff J, Phasukkijwatana N and Sarraf D, Developments in Ophthalmology **56**, 139 (2016).
- [9] Haitham N Zaatari, Nate J Kemp, Jesung Park, H G Rylander and Thomas E Milner, Retardation Measurement with Capillary Blood Flow using Enhanced Polarization-sensitivity Optical Coherence Tomography (EPS-OCT), Proceedings of SPIE **5690**, 228 (2005).
- [10] Amalendu Patnaik, R S Rengasamy, V K Kothari and A Ghosh, Textile Progress **38**, 1 (2006).
- [11] Myung Sup Yoon, Byoung Jae Kim and Hyung Jin Sung, International Journal of Heat and Fluid Flow **29**, 269 (2008).
- [12] Junya Ogawa, Isaku Kanno, Hidetoshi Kotera, Kiyotaka Wasa and Takaaki Suzuki, Sensors and Actuators A-physical **152**, 211 (2009).
- [13] Max E. Lippitsch, Sonja Draxler, Dietmar Kieslinger, Hartmut Lehmann and Bernhard H. Weigl, Applied Optics **35**, 3426 (1996).
- [14] Avik Dutt, Sudipta Mahapatra and Shailendra K. Varshney, Journal of the Optical Society of America B **28**, 1431 (2011).
- [15] V. G. Bar'yakhtar, L. E. Mikhailova, A. G. Il'inskii, A. V. Romanova and T. M. Khristenko, Zh. Eksp. Teor. Fiz. **95**, 1404 (1989).
- [16] G. Doge, Zeitschrift für Naturforschung **21A**, 266 (1966).